# Singlepion production cross sections at MiniBooNE

R. H. Nelson

Citation: AIP Conf. Proc. **1405**, 103 (2011); doi: 10.1063/1.3661567
View online: http://dx.doi.org/10.1063/1.3661567
View Table of Contents: http://proceedings.aip.org/dbt/dbt.jsp?KEY=APCPCS&Volume=1405&Issue=1
Published by the American Institute of Physics.

# Single-pion production cross sections at MiniBooNE

R. H. Nelson[1]

*Dept. of Physics, University of Colorado, Boulder; Boulder, CO 80309, USA*

**Abstract.** The MiniBooNE experiment has prepared an almost pure beam of muon-neutrinos over an energy range of a few-hundred MeV to a few GeV with a sample of roughly one-million neutrino interactions. Detailed cross-section measurements have been performed spanning 89% of the total neutrino-interaction rate. Specifically, three single-pion production mechanisms have been measured in detail. These measurements are important for a myriad of reasons: Neutral-current neutral-pion production is an important background for electron-neutrino appearance searches, Charged-current charged-pion production is the single largest background for quasi-elastic scattering and also provides the purest sample of events at these energies, and charge-current neutral-pion production provides a pure measure of incoherent pion production. Each of these processes required custom event reconstructions due to the particulars of the final-state particles. In addition, the sample selections and analyses will be discussed in detail. Many single-pion cross-section measurements, and their possible implications will be presented.

**Keywords:** Neutrinos, Pion production
**PACS:** 13.15.+g

## INTRODUCTION

The measurement of single-pion production cross sections has become the focus of recent experimental study in order to understand neutrino-nucleus interactions. The production of these pions, especially at low energy, has not been previously studied on nuclear targets. The interpretation of these measurements are further complicated by final-state interactions (FSI); the reinteractions of the particles produced in the initial neutrino-nucleon interaction with the spectator nucleons.

The Mini Booster Neutrino Experiment (MiniBooNE). [1, 2, 3] at Fermilab uses a focused $\nu_\mu$ beam over an energy from a few MeV to a few GeV with a peak energy around 700 MeV. This work focuses on MiniBooNE's pion production measurements [4, 5, 6]. MiniBooNE has measured 5 exclusive neutrino cross sections in detail [4, 5, 6, 7, 8] accounting for 89% of the total neutrino-interaction rate and 96% of the charged-current modes. The measurements of neutral-current single neutral-pion production (NC$\pi^0$), charged-current single neutral-pion production (CC$\pi^0$), and charged-current single charged-pion production (CC$\pi^+$) are discussed.

---

[1] Present Address: California Institute of Technology; Pasadena, CA 91125, USA

*NuInt11: The 7th International Workshop on Neutrino-Nucleus Interactions in the Few GeV Region*
AIP Conf. Proc. 1405, 103-108 (2011); doi: 10.1063/1.3661567

## MEASURING CROSS SECTIONS

Experimentally, measuring a cross section is rather straight forward. The differential cross section is given by

$$\frac{\partial \sigma}{\partial x_i} = \frac{\sum_j^{\text{bins}} U_{ij}(N_j - B_j)}{\varepsilon_i \phi_i n_{\text{targs}} \Delta x_i}, \tag{1}$$

where $N_j$ is the reconstructed number of events in bin $j$, $B_j$ is the predicted (or measured) number of background events in that bin, $U_{ij}$ is the element of the unfolding matrix mapping reconstructed quantities from bin $j$ to bin $i$, $\varepsilon_i$ is the efficiency, $\phi_i$ is the predicted flux for that bin[2], $n_{\text{targs}}$ is the number of interaction targets, and $\Delta x_i$ is the bin width. The reconstructed numbers of events and backgrounds come after all analysis cuts are applied. The unfolding matrix corrects out some model dependencies and the smearings associated with the reconstructions. Both the CC$\pi^0$ and CC$\pi^+$ analyses exclusively use the Bayesian unfolding method [9], while the unfolding methods vary for each of the NC$\pi^0$ measurements [4]. The efficiencies are estimated using the Monte Carlo (MC) and the neutrino flux prediction comes from Ref. [2]. The number of targets varies depending on whether the measurement is per nucleon (NC$\pi^0$), or per effective $CH_2$ mineral oil target (both CC$\pi^0$ and CC$\pi^+$).

### Observables vs. Inferables

A distinction should be made between directly observable quantities and "inferable" ones. An observable quantity is the least model-dependent measurement that can be made, usually as parameters returned directly from the event reconstructions. A inferable quantity is constructed using the base parameters and usually some assumptions. For the measurements presented here, only the neutrino cross section as a function of neutrino energy, $\sigma(E_\nu)$, and the flux-averaged cross section as a function of $Q^2$, $\partial\sigma/\partial Q^2$, are inferable quantities.

## EVENT RECONSTRUCTIONS

Each of the event reconstructions used for these analyses are based on the track-based event reconstruction described in detail in Ref. [10]. This is a maximum-likelihood method that fits for the energy, direction, and vertex of a particle-type hypothesis assuming that the particle traveled in a straight line and eventually stopped. Each set of these parameters generates a set of probability density functions (PDFs) for the expected charge and initial photon arrival time for each of the 1280 photomultiplier-tubes (PMTs) in the MiniBooNE detector. The PDFs were generated and parametrized by an extensive Monte Carlo simulation, and the parametrization allows for them to be calculated on-the-fly. The PDFs are dominated almost completely by the Cherenkov light with a small

[2] For the flux-averaged measurements $\phi_i \equiv \Phi$ where $\Phi$ is the total flux.

contribution due to the scintillation portion. The parameter set that maximizes the product of the probabilities is chosen as the fit values. The NC$\pi^0$ event reconstruction is also covered in Ref. [10] and is performed by fitting for the two photons from the $\pi^0$ decay simultaneously. The CC$\pi^+$ and CC$\pi^0$ event reconstructions build upon the track-based event reconstruction by extending to three tracks under certain hypotheses which will be discussed below.

The final state of an observable CC$\pi^+$ interaction contains a $\mu^-$, a $\pi^+$, and nuclear debris emanating from a common event vertex. To first order, the $\mu^-$ and $\pi^+$ are nearly indistinguishable by their Cherenkov light. This is because their masses are so similar. What can distinguish between the tracks are the occasional hadronic interactions of the $\pi^+$ which can cause it to suddenly change direction and lose some energy. The $\pi^+$ is fit by assuming that at some point the track changes direction and loses energy. The CC$\pi^+$ fitter then fits for two tracks from a common vertex, with a third track that begins at the end of one of the two tracks. This fitter is also helped by fixing the end points of the two particle tracks to the locations of the measured $\mu$-decay electrons ($\mu^- \rightarrow e^-$ and $\pi^+ \rightarrow \mu^+ \rightarrow e^+$). The nuclear debris is almost always below Cherenkov threshold at these particle energies and contributes only to the scintillation light. This fitting technique is discussed in detail in Refs. [6, 11].

For the CC$\pi^0$ fitter, three tracks are fit to a common event vertex: two photon tracks and one $\mu^-$ track. The photons, however, have an additional parameter to allow for the 67 cm conversion length in mineral oil. Rather than fix the end of the $\mu^-$ track to the $\mu$-decay electron the direction of the electron vertex is added as a pull-term in the likelihood calculation. This fitting technique is discussed in detail in Refs. [5, 12].

## EVENT SAMPLES

The stream of neutrino data is sorted based on low-level information garnered from the calibrated PMT measurements. First, as the neutrino beam is pulsed, the prompt interaction must occur during the beam time window. This rejects non-beam related events. Second, the events are sorted based on the total number of PMT hit clusters in time, or subevents. The first subevent of a neutrino interaction is due to the prompt neutrino interaction; all subsequent subevents are due to the electron from $\mu$-decays. Therefore, a simple counting of muons in the event plus the prompt interaction, gives the expected number of subevents: 1, 2, 3, for NC$\pi^0$, CC$\pi^0$, and CC$\pi^+$ events respectively. Next, a cut to remove stopped cosmic-ray muons that entered the detector before the start of data recording is made by requiring more than 200(175) PMT hits in the first subevent (175 was chosen for the CC$\pi^+$ analysis). The inverse of this cut is applied to the subsequent subevents to ensure that they are consistent with stopped muons. The last of these simple cuts demands that each subevent is contained within the inner detector volume by rejecting events with more than 6 PMT hits in the veto region for all subevents. Each analysis also employs slightly different fiducial volume cuts. All of these precuts, and the following analysis cuts are corrected for in the efficiency by the MC.

To further refine the NC$\pi^0$ sample a few additional cuts are applied. Events that are more $\mu$-like are rejected by cutting on the likelihood ratio of single-track electron to

muon fits as they tend to have no $\pi^0$s in the final state. The likelihood ratio of the $\pi^0$ two-track fit to the electron fit is used to reject single-track events. Finally, additional backgrounds are rejecting by selecting events with a well-reconstructed $\pi^0$ mass. After all cuts the NC$\pi^0$ sample contains 21375 candidate events at 75% purity and 36% efficiency. Additional information on the specific cut values can be found in Ref. [4].

The CC$\pi^+$ sample is the purest mode in the dataset after the application of the simple cuts specified above. In particular, the 3-subevent cut selects an extremely pure sample of observable CC$\pi^+$ events. The only additional cut on the sample rejects events with a poorly reconstructed resonance mass (dominated by the $\Delta(1232)$). Many of these events are expected to be background. After the addition of this cut there are 48322 candidate events with a 90% purity and a 12.7% efficiency. The loss in efficiency is mainly due to uncontained events and the fact that the muon capture rate on $CH_2$ is around 8% causing a significant fraction of CC$\pi^+$ to be 1-or 2-subevent events. Additional information can be found in Ref. [6].

The simple cuts listed above to select 2-subevent events is particularly good at finding the dominant $\nu_\mu$ charged-current quasi-elastic events (CCQE) as well as observable CC$\pi^0$ events. There are a factor of $\sim 10$ more CCQE than CC$\pi^0$ events in this sample. As the observable CC$\pi^0$ fit is fairly CPU intensive, the sample needs to be further reduced before the fit can be performed. A simple linear cut on the likelihood ratio of the one-track muon to electron fits versus the muon-fit energy is able to reject 98% of the $\nu_\mu$-CCQE events while keeping 86% of the CC$\pi^0$ events. This fitter occasionally places two of the tracks on top of one another making it difficult to distinguish which track is which. A cut is applied to reject tracks where the smallest angle between the three tracks is less than 0.6 radians. This cut is optimized to reject events with a mis-identified $\mu^-$ track. The second cut compares the likelihood ratio of the final-fit to a generic three-track fit where the particle types have not been specified. This cut rejects events without $\pi^0$s in the final state. The last cut selects well-reconstructed events by selecting event about the known $\pi^0$ mass. After all cuts there are 5810 candidate events with a 57% purity and 6.4% efficiency in the observable CC$\pi^0$ event sample. The largest background to this measurement are from CC$\pi^+$ interactions whose $\pi^+$ charged-exchanged or was absorbed by a different nucleus. The rate of CC$\pi^+$ production is fixed to the measured rate of observable CC$\pi^+$ production where it is then subtracted. Additional information can be found in Ref. [5].

## MEASUREMENTS

The single-pion measurements are summarized in Table 1. These measurements cover the full kinematics of the measured observable final-state particles (i.e. $\mu^-$, $\pi^0$, and $\pi^+$) as well as the inferable neutrino energy and $Q^2$ for the CC measurements. The observable differential cross-section measurements are the least model dependent of the set. Some of these measurements are distinctly different than NUANCE [13] implementation of the Rein-Sehgal model [14]. It should be noted that these measurements include FSI effects while many of the measurements that went into the Rein-Sehgal model were on hydrogen and deuterium and are not expected to have FSI. No attempt has been made to extract the FSI component from these cross sections. Fig. 1 summarizes the total

**TABLE 1.** Summary of the MiniBooNE single-pion production exclusive measurements. Each measurement is referenced by publication. The ⋆ denotes that the measurement is also presented as a function of neutrino energy. The † denotes that the cross sections were also measured in anti-neutrinos.

| Measurement | Mode NC$\pi^0$ | CC$\pi^0$ | CC$\pi^+$ |
|---|---|---|---|
| $\sigma(E_\nu)$ | | [5] | [6] |
| $\partial\sigma/\partial Q^2$ | | [5] | [6]⋆ |
| $\partial\sigma/\partial p_\pi$ | [4]† | [5] | [6]⋆ |
| $\partial\sigma/\partial \cos\theta_\pi$ | [4]† | [5] | [6]⋆ |
| $\partial\sigma/\partial T_\mu$ | | [5] | [6]⋆ |
| $\partial\sigma/\partial \cos\theta_\mu$ | | [5] | [6]⋆ |
| $\partial^2\sigma/\partial T_\mu \partial \cos\theta_\mu$ | | | [6] |
| $\partial^2\sigma/\partial T_\pi \partial \cos\theta_\pi$ | | | [6] |

cross sections of these single-pion production measurements. The NC$\pi^0$ measurement is single valued as only the flux-averaged total cross section can be extracted from the data.

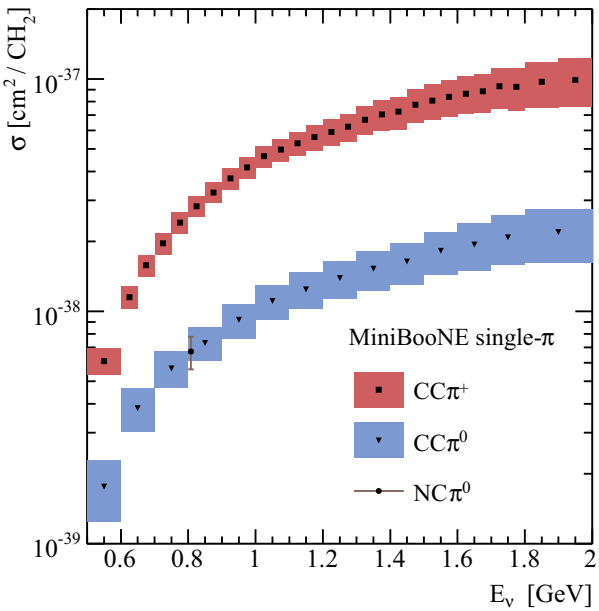


**FIGURE 1.** (color online) The total cross section as a function of neutrino energy for the CC$\pi^+$ (squares) and CC$\pi^0$ (triangles) measurements, and the flux-averaged total cross section for the NC$\pi^0$ (circle) measurement (scaled to a $CH_2$ target).

## CONCLUSIONS

A total of 18 cross-section measurements covering three important observable single-pion interactions have been presented [4, 5, 6]. These measurements cover the full kinematics of the observable final-state particles. They are a combination of the initial interaction cross section, FSI, and nuclear effects making them as model independent as possible. The cross sections, when presented this way, are most useful for experiments that attempt to predict their observable event rates for these modes.

## ACKNOWLEDGMENTS

The author would like to acknowledge the University of Colorado, the MiniBooNE collaboration, Fermilab, the U.S. Department of Energy, and the U.S. National Science Foundation. Additionally, this presentation would not have been possible without the invitation and support of the NuInt11 organizing committee.

## REFERENCES

1. E. Church, et al., A proposal for an experiment to measure $\nu_\mu \rightarrow \nu_e$ oscillations and $\nu_\mu$ disappearance at the Fermilab Booster: BooNE, http://www-boone.fnal.gov/publications/ (1997).
2. A. A. Aguilar-Arevalo, et al., *Phys. Rev. D.* **79**, 072002 (2009).
3. A. A. Aguilar-Arevalo, et al., *Nucl. Inst. Meth. A* **599**, 28 (2009).
4. A. A. Aguilar-Arevalo, et al., *Phys. Rev. D.* **81**, 013005 (2010).
5. A. A. Aguilar-Arevalo, et al., *Phys. Rev. D.* **83**, 052009 (2011).
6. A. A. Aguilar-Arevalo, et al., *Phys. Rev. D.* **83**, 052007 (2011).
7. A. A. Aguilar-Arevalo, et al., *Phys. Rev. D.* **81**, 092005 (2010).
8. A. A. Aguilar-Arevalo, et al., *Phys. Rev. D.* **82**, 092005 (2010).
9. G. D'Agostini, *Nucl. Instrum. Meth.* **A362**, 487–498 (1995).
10. R. B. Patterson, et al., *Nucl. Inst. Meth. A* **608**, 206 (2009).
11. M. J. Wilking (2009), FERMILAB-THESIS-2009-27.
12. R. H. Nelson (2010), FERMILAB-THESIS-2010-09.
13. D. Casper, *Nucl. Phys. Proc. Suppl.* **112**, 161–170 (2002).
14. D. Rein, and L. Sehgal, *Annals of Physics* **133**, 79 (1981).